Transcriptome differences between *Cupriavidus necator* NH9 grown with 3-chlorobenzoate and that grown with benzoate

Ryota Moriuchi
Shizuoka Daigaku
Hideo Dohra
Shizuoka Daigaku
Yu Kanesaki
Shizuoka Daigaku
Naoto Ogawa (ogawa.naoto@shizuoka.ac.jp)
Shizuoka Daigaku

Research article

Keywords: 3-chlorobenzoate, Aromatic degradation, Benzoate, Chemotaxis, Cupriavidus, RNA-seq, Stress response, Transcriptome, Transporter

Posted Date: November 10th, 2020

DOI: https://doi.org/10.21203/rs.3.rs-50641/v3

Version of Record: A version of this preprint was published at Bioscience, Biotechnology, and Biochemistry on March 15th, 2021. See the published version at https://doi.org/10.1093/bbb/zbab044.

Abstract

Background

Aromatic compounds derived from human activities are often released into the environment. Many of them, especially halogenated aromatics, are persistent in nature and pose threats to organisms. Therefore, the microbial degradation of these compounds has been studied intensively. Our laboratory has studied the expression of genes in *Cupriavidus necator* NH9 involved in the degradation of 3-chlorobenzoate (3-CB), a model compound for studies on bacterial degradation of chlorinated aromatic compounds. In this study aimed at exploring how this bacterium has adapted to the utilization of chlorinated aromatic compounds, we performed RNA-seq analysis of NH9 cells cultured with 3-CB, benzoate (BA), or citric acid (CA). The purpose of these analyses was to identify differentially expressed genes encoding products with various biological functions involved in the degradation of 3-CB and BA.

Results

Differential expression analysis confirmed strong induction of genes encoding enzymes in degradation pathways of 3-CB and BA, including *benABCD* (more than 256-fold compared with CA) encoding benzoate 1,2-dioxygenase involved in initial hydroxylation of both 3-CB and BA, and *cbnABCD* (more than 200-fold compared with BA and CA) encoding enzymes of chlorocatechol *ortho*-cleavage pathway. Four genes encoding major facilitator superfamily transporters were specifically induced by 3-CB or BA, and one cluster of genes encoding components of the ATP-binding cassette transporter system was significantly induced by 3-CB. Stress response genes encoding chaperones, proteases, the phosphate transporter PstBACS, and superoxide oxidase were upregulated in response to 3-CB and/or BA. Gene Ontology enrichment analysis revealed that genes encoding dioxygenases were upregulated by both 3-CB and BA. Intriguingly, the “cell motility,” “signal transduction,” and “chemotaxis” terms were significantly upregulated by BA compared with 3-CB. Consistent with this, in semi-solid agar plate assays, NH9 cells showed stronger chemotaxis to BA than to 3-CB.

Conclusions

Our results showed that the chemotaxis behavior of NH9 differs between 3-CB and BA. We inferred that NH9 has not fully adapted to the utilization of chlorinated benzoate, unlike its analogous aromatic compound BA, in nature.

Background

Aromatic compounds are one of the most widely distributed classes of organic compounds in nature. These compounds include aromatic amino acids, flavonoids, lignin components, and constituents of fossil fuels or compounds derived from human activities (e.g., dioxins and polychlorinated biphenyls: PCBs, etc.) [1, 2]. They are generally recalcitrant and persistent in the environment. Some of them are toxic to ecosystems or may be converted to hazardous products via natural processes. Therefore, these compounds should be removed promptly from the environment. Bioremediation is a process that utilizes the metabolic versatility of living organisms, mostly microorganisms and plants, to degrade or detoxify pollutants. Some microorganisms in soils and water can convert these organic chemicals to inorganic products [1-3]. To develop a useful strategy for the bioremediation of aromatic compounds, it is important to understand microbial behavior in response to such aromatic compounds and the molecular mechanisms underlying their decomposition by microorganisms.

Transcriptome analysis is an effective method to observe gene expression under different environmental conditions. Genome-wide expression profiling by DNA microarray analyses or next-generation sequencing techniques has been used to study many aromatic compound-degrading bacteria, including *Bacillus subtilis* NCIB 3610 (hydroxylated PCBs, methoxylated PCBs, and PCBs) [4], *Bradyrhizobium japonicum* USDA110 (4-hydroxybenzoate: 4-HBA, protocatechuate, vanillate, and vanillin) [5], *Comamonas testosteroni* WDL7 (3-chloroaniline) [6], *Cupriavidus pinatubonensis* JMP134 (2,4-dichlorophenoxyacetic acid: 2,4-D) [7], *Mycobacterium* sp. A1-PYR (phenanthrene and pyrene) [8], *Novosphingobium* sp. LH128 (phenanthrene) [9], *Paraburkholderia xenovorans* LB400 (benzoate: BA, biphenyl, PCBs, and phenylacetate) [10-13], *Pseudomonas putida* (3-chlorobenzoate: 3-CB and carbazole) [14-16], *Rhodococcus aetherivorans* I24 (biphenyl and PCBs) [17], *Rhodococcus jostii* RHA1 (BA, biphenyl, ethylbenzene, phthalate, and terephthalate) [18-20], *Sinorhizobium meliloti* 1021 (indole-3-acetic acid) [21], and *Sphingobium chlorophenolicum* L-1 (carbonyl cyanide *m*-chlorophenyl hydrazone, paraquat, pentachlorophenol, and toluene) [22]. Their results revealed differentially expressed genes (DEGs) involved in the degradation of aromatic compounds, stress responses, substrate transport, and transcriptional regulatory function. However, to our knowledge, no previous studies have tried to detect DEGs between a bacterium cultured with a simple chlorinated aromatic compound and its analogous aromatic compound without chlorine, and to get insight into bacterial adaptation to usage of chlorinated aromatic compound by integrating the abilities of chemotaxis, uptake and degradation of the compound.

Many members of the genus *Cupriavidus* in the family *Burkholderiaceae* are able to degrade aromatic pollutants [23-25]. For example, *Cupriavidus necator* strain NH9, isolated from a soil sample in Japan, can utilize 3-CB as carbon and energy source [26]. In our previous study,

we sequenced the genome of NH9 and identified genes involved in degradation pathways for aromatic compounds (including BA, catechol, and mono-hydroxylated benzoates) shared by several strains of the genus *Cupriavidus* [27]. Among the dozens of completely sequenced strains of *Cupriavidus*, strains NH9 [28], *Cupriavidus nantongensis* X1 [24], *Cupriavidus oxalaticus* X32 [25], and *C. pinatubonensis* JMP134 [23] have been reported to degrade chlorinated aromatic compounds. Also, in these strains, transcriptome analysis was performed only in strain JMP134 using 2,4-D, which focused on the expression of 2,4-D-degrading genes within mixed microbial communities [7]. There has been no report of analysis of whole transcriptome of *Cupriavidus* strains grown with chlorinated aromatic compound. This prompted us to investigate the differences in gene expression in NH9 between cells grown with 3-CB and those grown with its non-chlorinated counterpart, BA. In studies on microbial degradation, chlorobenzoates and BA have been used as model compounds for chlorinated and non-chlorinated aromatics, respectively, because of their simple structures [29, 30]. Chlorobenzoates are intermediate products in the bacterial degradation process of PCBs and are persistent in nature [29]. The results of this study reveal the differential gene expression profiles of strain NH9 between cells grown with 3-CB and those grown with BA. Our results imply that strain NH9 in the genus *Cupriavidus*, which is known to contain biodegrading strains, has not fully adapted to utilize chlorinated aromatic compounds, unlike natural aromatic compounds, in the environment.

Results

Growth of NH9 and its ability to degrade aromatic compounds

C. necator strain NH9 was grown on basal salts medium (BSM) containing 5 mM 3-CB, BA, or citric acid (CA). Strain NH9 was able to grow well with all three compounds although the growth rate was slightly lower with 3-CB than with BA and CA (Fig. 1A). High performance liquid chromatography (HPLC) analyses confirmed that both 3-CB and BA were completely degraded within 18 h of culture with NH9 (Fig. 1B). Compared with BA, 3-CB showed a slight time lag before degradation. Even after these compounds were decomposed thoroughly, the optical density at 600 nm (OD_{600}) did not decrease quickly.

Analysis of differentially expressed genes

To identify commonly and specifically expressed genes between NH9 cells cultured with 3-CB and those cultured with BA, we conducted transcriptome analyses. Reverse-transcribed ribosomal-RNA depleted RNA samples were sequenced on the Illumina MiSeq platform (Table S1). Prior to differential expression analysis, we evaluated similarities and variations in overall gene expression datasets among the samples. The biological replicates clustered closely in multi-dimensional scaling (MDS) plot and cluster dendrogram analyses (Fig. S1), indicative of very little variation among replicates. Genes that met the criteria of log fold-change (logFC) ≥ 2 or ≤ -2 with false discovery rate (FDR) < 0.05 were considered to be significantly differentially expressed between compared pairs of samples. First we compared the transcriptome of NH9 between cells grown with 3-CB and cells grown with BA. In total, 263 genes were expressed differentially: 137 genes were upregulated and 126 genes were downregulated in the 3-CB sample compared with the BA sample. In the 3-CB sample compared with the CA sample, 591 genes were expressed differentially: 374 were upregulated and 217 were downregulated. The largest number of DEGs was in this comparison. In the BA sample compared with the CA sample, 281 genes were differentially expressed: 228 were upregulated and 53 were downregulated. All differential expression analysis results are shown in Table S2.

Genes related to degradation of aromatic compounds

The genes involved in the degradation of 3-CB and BA and the logFC differences in their transcript levels between pairs of sample groups are shown in Table 1. The transcripts per million (TPM) values of each gene are shown in Figure 2. *benABCD* genes (Fig. S2A) were highly expressed in both the 3-CB and BA samples compared with the CA sample (logFC values 8.0 to 8.5). This is reasonable because BenABCD enzymes presumably react with both 3-CB and BA [31]. The chlorocatechol-degradation genes *cbnABCD* (Fig. S2B) [32] were strongly induced in the 3-CB sample (logFC values 9.4 to 9.9) but were also significantly expressed in the BA sample (logFC values 1.3 to 1.5). The genes *catA* (Fig. S2A), *catB*, *catDC* (Fig. S2C), and *pcaIJF* (Fig. S2D) encode products that participate in the degradation of catechol and 3-oxoadipate, respectively, and were expressed at almost the same levels in the 3-CB and BA samples. A Kyoto Encyclopedia of Genes and Genomes (KEGG) pathway analysis revealed that NH9 is able to decompose BA via another pathway, the epoxybenzoyl-CoA pathway [33], encoded by *bclA* and *boxABCD* genes (Fig. S2E and F). The *boxABCD* genes were upregulated in the BA sample compared with the CA sample. However, the transcript levels of *boxABCD* genes were lower than those of *ben* and *cat*.

In our previous study, analyses of the genome sequence of strain NH9 revealed genes involved in pathways that completely degrade 2-hydroxybenzoate (2-HBA), 3-hydroxybenzoate (3-HBA) (Fig. S2G), or 4-HBA (Fig. S2H) [27]. The transcript levels of the genes that putatively degrade these aromatic compounds were determined to ascertain whether 3-CB and BA affect their expression (Fig. S3 and Table S3). The transcript levels of the genes involved in the degradation of 2-HBA or 4-HBA were not very different between the CA sample and the 3-CB and

BA samples (only *pobA* in the BA sample was highly induced). Interestingly, the genes involved in the degradation of 3-HBA in NH9 (renamed from *nag* to *mhb*) [27] were significantly induced only by 3-CB.

Strain NH9 has genes related to anthranilate degradation on chromosome 1 (designated as *and1* or *andAc1Ad1Ab1Aa1*) (Fig. S2I). The products of those genes exhibit 43.9% to 73.3% amino acid sequence identities with the corresponding subunits of AndAcAdAbAa from *Burkholderia cepacia* DBO1, which is regulated by an AraC/XylS-type transcriptional regulator [34] (Fig. S4A). The presence of the complete set of genes for the initial degradation of anthranilate, together with *andR* encoding an AraC/XylS-type transcriptional regulator located upstream of the *and1* genes, suggests that this gene cluster is functional. Like the *mhb* genes above, *and1* was induced by 3-CB to a transcript level 8-fold that in the BA and CA samples (Fig. S3 and Table S3). Chromosome 2 also harbors putative *and* genes (designated as *and2* or *andAc2Ad2Ab2Aa2*) (Fig. S2J) and their transcript levels were significantly higher in the 3-CB sample than in the BA sample (Table S4). However, their amino acid sequence identities with the corresponding subunit of AndAcAdAbAa from *B. cepacia* DBO1 were found to be lower than 45% (Fig. S4A). Also, the putative transcriptional regulator located close to the degradation genes was a member of the MarR family, rather than being an AraC/XylS-type regulator. Therefore, it is difficult to speculate whether *and2* genes are involved in anthranilate degradation or not.

Transporters

The KEGG BRITE functional classification of strain NH9 revealed that 348 genes encode proteins with transporting functions ("Transporters," ko02000). Of these 348 genes, those that were upregulated (logFC $\geq$ 2 and FDR < 0.05) by 3-CB and/or BA encoded eight major facilitator superfamily (MFS) transporters and 12 sets of ATP-binding cassette (ABC) transporters. This analysis identified the transporters induced by 3-CB and/or BA (Table 2).

Of the eight MFS transporter genes mentioned above, BJN34_12320, BJN34_18155, and BJN34_30890 had higher transcript levels in the 3-CB sample than in the BA sample, and BJN34_32125 showed the opposite result. The logFC values of the other four genes were not significantly different between 3-CB vs. CA and BA vs. CA. A BLASTP analysis was performed to compare the amino acid sequences of the eight transporters of NH9 with those that have been experimentally verified or functionally analyzed (Table S5). The products of BJN34_18155 and BJN34_32125 exhibited more than 70% amino acid sequence identities with BenP (a 3-CB transporter) [35]. The products of BJN34_30890 and BJN34_33870 showed moderate identities (>50%) with MhbT (a 3-HBA transporter) [36] and PcaK (a 4-HBA transporter) [37, 38], respectively (Table 2). Phylogenetic analysis of the eight MFS transporters of NH9 together with other known MFS transporters confirmed the close relationships of the four transporters mentioned above with their counterparts in other species, and grouped them in the aromatic acid:H^+ symporter (AAHS) family of MFS (Fig. 3). Three other transporters (products of BJN34_11715, BJN34_12320, and BJN34_26825) belonged to the anion/cation symporter (ACS) family and the product of BJN34_20520 belonged to the metabolite:H^+ symporter (MHS) family. We then explored the genes surrounding the eight MFS transporter-encoding genes in the NH9 genome, and found that BJN34_32125, BJN34_30890, BJN34_33870, and BJN34_18155 were located next to clusters of genes related to the degradation of BA, 3-HBA, 4-HBA, and anthranilate, respectively (Fig. S2F, G, H, and I). No clusters of genes involved in degradation of aromatic compounds were located around the genes encoding the other four MFS transporters.

Our results showed that 3-CB and BA induced many genes encoding ABC transporters in NH9 (Table 2). The logFC values of most ABC transporter genes were similar between 3-CB vs. CA and BA vs. CA. However, BJN34_29445 to BJN34_29465 were clearly overexpressed in the 3-CB sample, suggesting that these genes were induced specifically by 3-CB. These gene products showed 27.7% to 40.3% amino acid sequence identities with Pca proteins, which are involved in 3,4-dihydroxybenzoate transport [39]. Transporters in other families were also identified in the BLASTP analysis (Table S6). Although a few genes (e.g., BJN34_08680 and BJN34_26835) were differentially expressed in response to both 3-CB and BA, most genes did not show significant changes in their transcript levels, or were downregulated, in either the 3-CB or BA samples compared with the CA sample.

Stress responses

Stress response genes were upregulated when NH9 cells were cultured with 3-CB and BA (Table S4). Four genes encoding molecular chaperones, *dnaK* (BJN34_09490), *groEL* (BJN34_09495), *groES* (BJN34_09500), and *clpB* (BJN34_11475) were significantly upregulated more than 2-fold by both 3-CB and BA compared with CA. *hslV* (BJN34_00915), *hslU* (BJN34_00920), *grpE* (BJN34_06000), and *dnaK* (BJN34_16500) were induced only by BA (FDR < 0.05). We also searched for the genes in strain NH9 corresponding to the aromatics stress response genes identified in the previous study [40] in the KEGG database, and their expression patterns are summarized in Table S4 (categorized as "Benzoate stress response genes"). Only the genes encoding the phosphate transporter PstBACS (BJN34_13095 to BJN34_13110) and superoxide oxidase (SOO) (BJN34_16665) were induced by 3-CB and BA, respectively.

Functional changes

To detect changes in biological function, we conducted Gene Ontology (GO) enrichment analysis by the parametric analysis of gene set enrichment (PAGE) method based on logFC values. The comparisons of 3-CB vs. CA, BA vs. CA, and 3-CB vs. BA detected enrichment of 22, 22, and 15 GO terms, respectively, with FDR < 0.05 (Fig. 4 and Table S7). The GO terms “ferric iron binding” (GO:0008199), “metal ion binding” (GO:0046872), and “2 iron, 2 sulfur cluster binding” (GO:0051537) were significantly upregulated only in the 3-CB sample. On the contrary, the GO terms “nucleotide binding” (GO:0000166) and “peptidyl-prolyl cis-trans isomerase activity” (GO:0003755) were significantly downregulated only in the 3-CB sample. In the BA sample specifically, the GO terms “peptide transport” (GO:0015833) and “bacterial-type flagellum-dependent cell motility” (GO:0071973) were significantly upregulated and “GTPase activity” (GO:0003924), “porin activity” (GO:0015288), and “oxidoreductase activity, acting on the CH-OH group of donors, NAD or NADP as acceptor” (GO:0016616) were significantly downregulated. Interestingly, “chemotaxis” (GO:0006935), “signal transduction” (GO:0007165), and “bacterial-type flagellum-dependent cell motility” (GO:0071973) were downregulated in the 3-CB sample compared with the BA sample. The trends in the variations of the other GO terms listed in Fig. 4 and Table S7 were similar between 3-CB vs. CA and BA vs. CA.

The induction or repression of genes in the “signal transduction,” “chemotaxis,” and “bacterial-type flagellum-dependent cell motility” categories in response to 3-CB, BA, and CA is summarized in Table S8. The 72 genes in the “signal transduction” category mainly encoded proteins related to bacterial chemotaxis and a histidine kinase. Crucially, this category included 12 genes encoding methyl-accepting chemotaxis proteins (MCPs), which play key roles in sensing extracellular signals [41, 42]. Eight of 12 MCP genes were DEGs in the 3-CB vs. BA comparison, and were downregulated in the 3-CB sample. Because three of these eight genes (BJN34_09575, BJN34_21800, and BJN34_32190) were upregulated more than 2-fold with FDR < 0.05 by BA compared with CA, it is likely that their products detect BA or related chemicals as ligands. One MCP gene (BJN34_24350) was significantly upregulated more than 16-fold by both 3-CB and BA compared with CA, indicating that it responded to 3-CB and BA or their related chemicals. In the “chemotaxis” category, many genes were classified as “signal transduction.” Seven of 16 genes were DEGs in the 3-CB vs. BA comparison, and six of them were upregulated more than 2-fold (FDR < 0.05) by BA compared with CA. These six genes encoded CheABDVW proteins and a MCP. Of the 14 genes in the “bacterial-type flagellum-dependent cell motility” category, 11 were upregulated more than 2-fold (FDR < 0.05) by BA compared with CA. These genes encoded proteins comprising the flagellum: the hook, hook-filament junction, distal rod, proximal rod, L ring, P ring, and a part of the C ring. Our data indicated that the genes encoding MCP, Che, and components of the flagellum in NH9 were upregulated by BA and downregulated or not affected by 3-CB. This was predicted to result in differences in cell motility or chemotaxis functions of NH9 cells between 3-CB and BA.

Chemotactic response toward aromatic compounds

To determine whether the transcriptional responses of chemotaxis genes corresponded to actual differences in chemotaxis behavior towards 3-CB and BA, we performed semi-solid agar plate assays (Fig. 5). The formation of a concentric ring was a positive response, as it was indicative of the accumulation of bacterial cells encircling the attractant. NH9 cells formed clear migrating rings around casamino acids (positive control) and BA within 3 and 6 h, respectively (Fig. 5A and B). In contrast, NH9 cells formed a migrating ring only weakly around 3-CB after 14 h (Fig. 5C). There was no ring around BSM without any carbon source (negative control) (Fig. 5D). These results confirmed that strain NH9 has a strong chemotactic response towards BA but a weak response towards 3-CB.

Discussion

In this study, the results of transcriptome analysis of the cells of NH9 grown with 3-CB, BA, and CA showed differential expression patterns depending on the substrate. While the expression patterns of the genes involved in the degradation of 3-CB and BA were highly upregulated in agreement with our expectation, some of the genes involved in transport and chemotaxis were differentially regulated between 3-CB and BA, which suggested different level of adaptation of NH9 to the two compounds (see below).

The RNA-seq analyses confirmed that genes related to 3-CB and BA metabolism are expressed in NH9, as predicted in a previous study [27]. The *cbnABCD* genes encoding enzymes involved in 3-chlorocatechol degradation were upregulated in NH9 cells grown with 3-CB and BA, especially 3-CB (Table 1 and Fig. 2). In NH9 cells grown with 3-CB and BA, *benABCD* and *catA* were upregulated, presumably as a result of the action of the LysR-type transcriptional regulator (BJN34_08550) (Fig. S2A). These results are consistent with the degradation pathways of the two compounds. *catB* and *catDC* were upregulated in NH9 cells in the presence of either 3-CB or BA and are located on a different chromosome from *benABCD* and *catA*. While the expression of the *catB* gene could be regulated by the product of BJN34_24335 encoding a LysR-type transcriptional regulator, a transcriptional regulator of *catDC* genes could not be estimated (Fig. S2C). The *boxABCD* genes encoding enzymes involved in BA degradation were upregulated in BA compared with CA, but the transcript levels of them were lower than those of *ben* and *cat* genes (Table 1 and Fig. 2). These results suggested that, in these experimental conditions, NH9 may primarily degrade BA via the route involving *ben* and *cat* genes, rather than the route involving *benA* and *boxABCD* genes.

C. necator NH9 consumed both 3-CB and BA within 18 h, when growth apparently reached the stationary phase (Fig. 1). However, even after aromatic compounds were completely degraded, the OD_{600} of the culture did not decrease during a further 30 h. When strain NH9 was

cultured with CA, the curve showed a similar trend. This is probably due to the accumulation and consumption of the biodegradable polyester, polyhydroxybutyrate (PHB). PHB is naturally synthesized as a carbon reserve storage material from acetyl-CoA, which is metabolite of both 3-CB and BA, under nutrient limitation and stress conditions [43]. *Cupriavidus necator* strain H16 has been studied intensively as a PHB producer. The genome of H16 contains classic PHB synthesis genes (*phaC$_1$AB$_1$* operon) that are distributed and conserved among members of the genus *Cupriavidus* [44, 45]. The genome of strain NH9 also contains *pha* The proteins encoded by these genes showed more than 93% amino acid identities with those of H16. In the present study, these *pha* genes were expressed at higher levels than the housekeeping gene *gyrB* in all cultures, regardless of the substrate (Tables S2 and S4), suggesting that PHB synthesis occurred under these conditions.

The products of *mhbDHIMT* genes in strain NH9 showed high identities (52.1% to 71.9% identity at the amino acid level) with those involved in the degradation of 3-HBA in *Klebsiella pneumoniae* M5a1 (Fig. S4B). A previous study on strain M5a1 reported that the expression of *mhb* degradation genes is regulated by *mhbR* (located upstream), which is induced by 3-HBA [46]. We conducted growth experiments and qRT-PCR analyses of NH9 cells grown with 3-HBA as the substrate and obtained the following results: (i) NH9 cells were able to use 3-HBA as the sole source of carbon and energy; and (ii) the *mhbDHIMT* genes in NH9 were highly induced by 3-HBA (data not shown). These results strongly suggest that *mhbDHIMT* genes in strain NH9 are involved in the degradation of 3-HBA and are induced by 3-HBA, consistent with the *mhb* genes in *K. pneumoniae* M5a1. In this study, 3-CB was found to upregulate the expression of *mhbDHIMT* genes in strain NH9 (Fig. S3 and Table S3). Thus our results imply that MhbR in NH9 recognized not only 3-HBA but also 3-CB (or its intermediate metabolite) as an inducer to activate the transcription of *mhbDHIMT* genes. The putative anthranilate decomposition genes (*and1* and *and2*) were also upregulated by 3-CB but not by BA (Fig. S3, Tables S3, and S4). Although anthranilate is structurally more different from 3-CB than 3-HBA is, the transcriptional regulator of anthranilate degradation genes in NH9 may recognize 3-CB (or its intermediate metabolite) as an inducer.

Many candidate genes involved in the transport of 3-CB and/or BA were identified via the KEGG BRITE functional classification and BLASTP analyses (Tables 2 and S6). Because BJN34_18155 and BJN34_32125 are evolutionarily close to BenP, a MFS transporter involved in 3-CB uptake in *C. pinatubonensis* JMP134 [35] (Fig. 3), their products may be involved in 3-CB import in NH9. BJN34_18155, BJN34_30890, BJN34_32125, and BJN34_33870, which encode MFS transporters, may be involved in the transport of anthranilate, 3-HBA, BA, and 4-HBA, respectively, because each of these genes is located in a cluster of genes related to degradation of each respective compound (Fig. S2F, G, H, and I). Genes encoding components of the ABC transport system (BJN34_29445 to BJN34_29465) were more strongly expressed in NH9 cells grown with 3-CB than in NH9 cells grown with BA or CA. As far as we know, the ABC transporter that imports 3-CB into cytoplasm has not been reported yet. The products of BJN34_29445 to BJN34_29465 may be components of a novel 3-CB transporter. Intriguingly, a gene related to anthranilate degradation (*and2*) was located next to BJN34_29445 to BJN34_29465, and was significantly induced by 3-CB (Fig. S2J and Table S4). Thus, this ABC transporter system may be originally involved in importing anthranilate. Aromatic compounds are taken up by members of the MFS and ABC families, but also by members of other transporter families [47-50]. However, our results indicate that the MFS and ABC family transporters listed in Table 2 could play key roles in importing 3-CB and BA into NH9 cells.

The stress response genes with altered expression included those encoding molecular chaperones (DnaK, GrpE, GroESL, and ClpB) and proteases (HslVU) (Table S4). Previous studies have shown that these proteins are rapidly induced under various stress conditions such as salt, acid, heat, cold and oxidative stress [51]. In NH9, genes encoding either chaperones or proteases might be upregulated to refold misfolded proteins and to decrease the harmful impact of protein aggregation in the presence of aromatic compounds (Table S4). In another study, the stress responses of *P. putida* KT2440 to 45 mM BA were analyzed by global mRNA expression profiling and several genes were identified as stress response genes [40]. We expected that the genes induced by BA in strain KT2440 are also upregulated by 3-CB and/or BA in strain NH9, however more than half of investigated genes were downregulated by 3-CB and BA compared with CA (Table S4) and genes encoding the phosphate transporter PstBACS and superoxide scavenger SOO [52] were induced by 3-CB and BA, respectively in NH9. The previous study estimated that intracellular phosphate is a buffer for neutralizing the BA and is used in the synthesis of membrane constituents and energy-rich intermediates [40]. Presumably, PstBACS coding genes might be upregulated to maintain the intracellular pH disturbed by 3-CB. The degradation of aromatic compounds by oxygenases can generate reactive oxygen species (ROS) which damage various cellular components such as DNA, proteins, and lipids in aerobic organisms [22, 53] and upregulate various stress response genes [15, 17, 54]. This study suggested that SOO coding genes were also induced to solve ROS accumulation.

The four GO terms, “cellular aromatic compound metabolic process,” “iron ion binding,” “2 iron, 2 sulfur cluster binding,” and “ferric ion binding” were upregulated by 3-CB and BA compared with CA. In particular, 3-CB induced the expression of many genes encoding dioxygenases (Fig. 4 and Table S7). Dioxygenases contain two conserved regions: the Rieske [2Fe-2S] cluster and the mononuclear iron-containing catalytic domain. These enzymes play a critical role in initiating the biodegradation of a variety of aromatic compounds under aerobic conditions [55]. Upregulation of these functions, including dioxygenase activity, would be conducive to the degradation of aromatic pollutants.

Notably, NH9 cells showed stronger chemotaxis towards BA than towards 3-CB, as demonstrated in the semi-solid agar plate assays (Fig. 5). This was consistent with the upregulation of chemotaxis genes by BA compared with 3-CB. The predicted chemotaxis pathway of strain NH9 towards BA is described below and depicted in Fig. 6. To initiate the typical chemotactic response, MCPs first detect their ligands [41]. In strain NH9, among 12 genes encoding MCPs, at least four, BJN34_09575 (K05874), BJN34_21800 (K05874), BJN34_24350 (K05874), and BJN34_32190 (K03406), encode products that could function as receptors for BA or related chemicals. Binding of an attractant induces a conformational change in MCPs such that they transfer a phosphate group from the histidine kinase CheA (BJN34_21875) to the response regulator CheY [42]. The NH9 genome contains two *cheY* genes (BJN34_21830 and BJN34_21900) that were significantly upregulated by BA and downregulated by 3-CB (Table S2). The phosphorylated CheY interacts with switch proteins in the flagellar motor such as FliM (BJN34_24450) [56], FliN (BJN34_24445) [57] and FliG (BJN34_34155) [58]. As a result, the swimming behavior of bacterial cells migrates towards BA. The upregulation of the complete set of genes required for chemotaxis strongly suggests that their products are involved in chemotaxis to BA.

Among the few transporters reported to transport of chlorinated aromatic compounds, TfdK of *C. pinatubonensis* JMP134 is encoded by a gene located at the downstream end of a gene cluster involved in 2,4-D degradation. This protein is reported to be involved in both the uptake of, and chemotaxis to, 2,4-D [59, 60]. This tendency for genes with related functions to cluster together is considered to be the result of evolution [61]. It has been observed for many genes encoding MFS transporters of aromatic compounds commonly found in nature, for example, *pcaK,* which is involved in the uptake of, and chemotaxis to, 4-HBA in *P. putida* [62], and *benK,* which is involved in the uptake of BA in *Acinetobacter baylyi* ADP1 [63]. In contrast, the genes involved in uptake of/chemotaxis to 3-CB in bacteria have remained elusive. That is, the genes that are presumed to be responsible for these functions are not located adjacent to genes involved in 3-CB degradation (encoding front-end enzymes, benzoate 1,2-dioxygenase and *cis*-diol dehydrogenase, and enzymes involved in chlorocatechol *ortho*-cleavage pathway). *C. pinatubonensis* strain JMP134 utilizes 3-CB as well as 2,4-D. However, in strain JMP134, *benP* (encoding a protein involved in 3-CB uptake) is not located on the plasmid pJP4 that contains genes related to the degradation of 2,4-D and chlorocatechols converted from 3-CB, but is located on the chromosome [35]. With regard to chemotaxis to 3-CB, the presence of ICE*clc* in strain B13 was found to be related to the upregulation of genes involved in flagellar assembly and increased swimming motility [16]. A B13 strain that did not contain ICE*clc*, but only the chlorocatechol degradation genes, did not show upregulation of swimming motility. The upregulation in the ICE*clc*-containing strain was suggested to be mediated by a gene located in ICE*clc*, *orf2848*, which is homologous to *pcaK* [16]. In the present study, the genes encoding transporters that were upregulated by 3-CB were located on chromosomes either discretely or together with genes related to the degradation of aromatic compounds such as 3-HBA and anthranilate (Fig. S2G, I, and J), but were not closely located to genes involved in 3-CB degradation (encoding the front-end enzymes and the enzymes for chlorocatechol degradation). This raises several possibilities: 1. Utilization of 3-CB does not require increased expression of specific transporter (s), and the transporter genes that were upregulated in NH9 cells grown with 3-CB were fortuitously upregulated. 2. While 3-CB strongly induces genes encoding front-end enzymes including benzoate 1,2-dioxygenase, the gene (s) related to BA uptake are insufficient for 3-CB uptake. Therefore, other transporter genes, such as those upregulated in our study, are induced to complement this function. Because the substrate specificity of aromatic compound transporters is not known, either of these possibilities may explain the uptake of 3-CB. However, if we include chemotaxis (which may be linked to uptake) when considering the behavior of NH9 towards 3-CB (Fig. 5), our results show that NH9 has weaker chemotaxis towards 3-CB than towards BA. This fact, combined with the absence of closely located genes related to uptake/chemotaxis, strongly suggests that strain NH9 does not utilize 3-CB as efficiently as it utilizes BA in the environment. In our experiments, NH9 also showed strong chemotaxis towards 3-HBA (data not shown), providing further evidence that this strain is adapted for utilization of aromatic compounds commonly found in nature.

Conclusion

We examined transcriptome differences in *C. necator* strain NH9 between cells cultured with 3-CB and those cultured with BA. The RNA-seq analyses revealed more changes in gene expression in response to 3-CB than to BA. The trends in differential gene expression were similar, but genes related to the degradation of particular aromatic compounds (3-chlorocatechol, BA, 3-HBA, and anthranilate) showed differences in transcript levels among the various treatments. The genes encoding transporters (MFS and ABC type), components of the stress response, flagellar proteins, and chemotaxis proteins also showed differences between 3-CB and BA. The chemotaxis response of NH9 cells showed the biggest difference between 3-CB and BA. The substrate BA markedly upregulated certain genes related to the chemotaxis response, but 3-CB did not, consistent with the chemotaxis behavior observed in semi-solid agar assays. Together, our findings suggest that NH9 has not fully adapted to utilization of chlorinated benzoate, unlike its analogous aromatic compounds such as BA.

Methods

Bacterial strain, culture media, and growth experiment

C. necator stain NH9 was grown on BSM [26] supplemented with 5 mM 3-CB, BA, or CA at 30 °C. All the chemical reagents for media were purchased from Fujifilm-Wako (Osaka, Japan). Strain NH9 from glycerol stock was inoculated onto BSM agar medium containing the respective carbon source and incubated for 2 days. Subsequently, the cells were precultured in liquid medium containing the respective carbon source with shaking at 120 rpm for 24 h. Then, a portion of each preculture was inoculated into fresh culture medium containing the corresponding carbon source. The amount of the volume of the preculture to be inoculated to the fresh medium was adjusted so that OD_{600} of the successive culture was 0.01 at the starting point. Also, the volume of the successive culture was adjusted to 100 ml. For the growth experiment, cultures were shaken at 120 rpm and the OD_{600} was monitored using an Ultrospec 3000 spectrophotometer (Amersham Pharmacia Biotech, Piscataway, NJ, USA).

HPLC analysis to quantify aromatic compounds

For the HPLC analysis, 300 µl NH9 cell culture was collected and 100 µl methanol was added to stop bacterial growth. The mixture was vortexed and then centrifuged at 9,100 × *g* for 3 min at 4 °C. The supernatant was filtered through a 0.2-µm pore-size hydrophilic PTFE membrane filter (Merck Millipore, Burlington, MA, USA) and then subjected to HPLC analysis using a SCL-10A VP system (Shimadzu, Kyoto, Japan) equipped with a YMC-Triart C18 column (150 mm × 4.6 mm, 5 µm; YMC, Kyoto, Japan). Water-acetonitrile-acetic acid was used as the mobile phase for analysis of 3-CB (45:50:5, v/v) and BA (75:20:5, v/v). The flow rate was 1 ml min^{-1} and the column temperature was held constant at 37 °C. A SPD-10AVi wavelength detector (Shimadzu) was used to detect 3-CB at 200 nm and BA at 254 nm. The concentrations of aromatic compounds were calculated from calibration curves.

Total RNA extraction, cDNA library preparation, and RNA-sequencing

The NH9 cells from three biologically independent cultures with each of the three carbon sources were harvested at mid-growth phase (OD_{600} = 0.2 to 0.5). The cells were collected by centrifugation (10,000 × *g* for 5 min at 4 °C) and immediately treated with RNAprotect Cell Reagent (QIAGEN, Hilden, Germany). The cells were collected by centrifugation (8,000 × *g* for 10 min at room temperature) and then stored at −80 °C until RNA isolation. Total RNA was extracted using the RNeasy Mini Kit (QIAGEN), and contaminating DNA was removed by two treatments with the Turbo DNA-free Kit (Thermo Fisher Scientific, Waltham, MA, USA) following the manufacturer's instructions. The genomic DNA-depleted RNA was further purified using the RNeasy Mini Kit following the supplementary protocol. The quantity of the purified total RNA was measured by fluorometry using the Qubit RNA HS Assay Kit (Thermo Fisher Scientific), and the quality of the purified total RNA was assessed using an Agilent 2100 Bioanalyzer (Agilent Technologies, Santa Clara, CA, USA), and TECAN Infinite M200 (TECAN, Mannedorf, Switzerland) or Varioskan LUX (Thermo Fisher Scientific) plate readers. Ribosomal RNA was removed from 5 µg purified total RNA using the Ribo-Zero rRNA Removal Kit for Gram-negative bacteria (Illumina, San Diego, CA, USA), and the resultant mRNA was purified using the RNeasy MinElute Cleanup Kit (QIAGEN) for cDNA synthesis. Subsequently, cDNA libraries were prepared with 50 ng mRNA using the KAPA Stranded mRNA-Seq Kit (Kapa Biosystems, Woburn, MA, USA) according to the manufacturer's instructions, including the skipping mRNA capture protocol. The indexed cDNA libraries were pooled and sequenced on a MiSeq system (Illumina) with 76-bp paired-end reads at the Instrumental Research Support office, Research Institute of Green Science and Technology, Shizuoka University, Japan. See Table S1 for detailed information about RNA-seq read data.

Mapping, read counts, and differential expression analysis

The obtained raw reads were filtered with Trimmomatic version 0.36 [64]. Adapter sequences, the terminal 76 bases, low-quality reads of < Q15, and reads of < 50 bp were trimmed. The cleaned reads were mapped to the NH9 complete genome sequence (accession no. P017757 to CP017760) using HISAT2 version 2.1.0 [65] with report alignments option (–dta) and strand-specific option (–rna-strandness RF). The number of aligned reads was counted and TPM values were calculated using StringTie version 1.3.5 [66] with strand option (–rf). Read counts data for differential expression inputs were generated using the prepDE.py script (http://ccb.jhu.edu/software/stringtie/dl/prepDE.py). The DEGs were identified using edgeR package version 3.24.3 [67].

GO enrichment analysis

All proteins were annotated by hmmscan (http://hmmer.org/) against the Pfam database release 32.0 [68]. The Pfam IDs were converted into GO terms using the pfam2go conversion table (http://current.geneontology.org/ontology/external2go/pfam2go) [69]. The PAGE method [70] was used to detect a large number of significantly altered gene sets and functions. GO terms with FDR < 0.05 were considered statistically significant.

Semi-solid agar plate assays

The chemotactic behavior of strain NH9 towards aromatic compounds was tested in semi-solid agar plate assays [71]. For these assays, 100 ml NH9 cell culture in the early stationary phase ($O.D._{600}$ ~0.8) was centrifuged (1,600 × *g* for 5 min at 4 °C), then the pelleted cells were

washed twice with BSM and resuspended in 25 ml BSM containing 0.2% (w/v) agar. Aliquots (5 ml) of resuspended cells were poured into 60-mm-diameter plastic Petri plates. Then, an 8-mm-diameter filter paper disk that was spotted with 20 µl 500 mM 3-CB or BA, or a 5% (w/v) solution of casamino acids (positive control), was placed in the center of each Petri plate. In the negative control, filter paper was spotted with 20 µl BSM without any carbon source. The chemotactic response was observed after 3 to 14 h of incubation at 25 °C.

Declarations

Ethics approval and consent to participate

Not applicable.

Consent for publication

Not applicable.

Availability of data and material

All data generated or analyzed during this study are available from the corresponding author upon reasonable request. Raw data sequences generated in the current study have been submitted to the DDBJ Sequence Read Archive (DRA) under the accession no. DRR232374 to DRR232382.

Competing interests

The authors declare that they have no competing interests.

Funding

This work was partially supported by JSPS KAKENHI (Grant-in-Aid for Scientific Research (C)), grant number 26450087. The funding body were not involved in study design, data collection and analysis, interpretation of data, and preparation of the manuscript.

Authors' contributions

RM and NO conceived and designed the experiments. RM performed the experiments, analyzed and interpreted the data, and wrote the manuscript. HD and YK provided assistance with analytical tools. HD, YK, and NO critically reviewed the manuscript. NO is responsible for the project.

Acknowledgements

The authors thank Mr. Ayumu Wada (Nippon Paper Industries Co., Ltd.) for his valuable comments. We also thank Dr. Kimiko Yamamoto-Tamura (Institute for Agro-Environmental Sciences, NARO) for her helpful advice for the semi-solid agar plate assay.

Abbreviations

2,4-D, 2,4-dichlorophenoxyacetic acid; 3-CB, 3-chlorobenzoate; AAHS, aromatic acid:H^+ symporter; ABC, ATP-binding cassette; ACS, anion/cation symporter; BA, benzoate; BSM, basal salts medium; CA, citric acid; DEGs, differentially expressed genes; FDR, false discovery rate; GO, gene ontology; HBA, hydroxybenzoate; HPLC, high performance liquid chromatography; KEGG, Kyoto Encyclopedia of Genes and Genomes; LogFC, log fold-change; MCP, methyl-accepting chemotaxis protein; MDS, multi-dimensional scaling; MFS, major facilitator superfamily; MHS, metabolite:H^+ symporter; OD_{600}, optical density at 600 nm; PAGE, parametric analysis of gene set enrichment; PCBs, polychlorinated biphenyls; PHB, polyhydroxybutyrate; ROS, reactive oxygen species; SOO, superoxide oxidase; TPM, transcripts per million.

References

1. Carmona M, Zamarro MT, Blázquez B, Durante-Rodríguez G, Juárez JF, Valderrama JA, Barragán MJ, García JL, Díaz E. Anaerobic catabolism of aromatic compounds: a genetic and genomic view. Microbiol Mol Biol Rev. 2009;73(1):71-133.
2. Seo JS, Keum YS, Li QX. Bacterial degradation of aromatic compounds. Int J Environ Res Public Health. 2009;6(1):278-309.
3. Alexander M. Biodegradation of chemicals of environmental concern. Science. 1981;211(4478):132-8.
4. Sun J, Pan L, Zhu L. Formation of hydroxylated and methoxylated polychlorinated biphenyls by *Bacillus subtilis*: New insights into microbial metabolism. Sci Total Environ. 2018;613-614:54-61.

5. Ito N, Itakura M, Eda S, Saeki K, Oomori H, Yokoyama T, Kaneko T, Tabata S, Ohwada T, Tajima S, Uchiumi T, Masai E, Tsuda M, Mitsui H, Minamisawa K. Global gene expression in *Bradyrhizobium japonicum* cultured with vanillin, vanillate, 4-hydroxybenzoate and protocatechuate. Microbes Environ. 2006;21(4):240-50.
6. Wu Y, Mohanty A, Chia WS, Cao B. Influence of 3-chloroaniline on the biofilm lifestyle of *Comamonas testosteroni* and its implications on bioaugmentation. Appl Environ Microbiol. 2016;82(14):4401-9.
7. Dennis P, Edwards EA, Liss SN, Fulthorpe R. Monitoring gene expression in mixed microbial communities by using DNA microarrays. Appl Environ Microbiol. 2003;69(2):769-78.
8. Yuan K, Xie X, Wang X, Lin L, Yang L, Luan T, Chen B. Transcriptional response of *Mycobacterium* sp. strain A1-PYR to multiple polycyclic aromatic hydrocarbon contaminations. Environ Pollut. 2018;243(Pt B):824-32.
9. Fida TT, Moreno-Forero SK, Breugelmans P, Heipieper HJ, Röling WF, Springael D. Physiological and transcriptome response of the polycyclic aromatic hydrocarbon degrading *Novosphingobium* sp. LH128 after inoculation in soil. Environ Sci Technol. 2017;51(3):1570-9.
10. Denef VJ, Park J, Tsoi TV, Rouillard JM, Zhang H, Wibbenmeyer JA, Verstraete W, Gulari E, Hashsham SA, Tiedje JM. Biphenyl and benzoate metabolism in a genomic context: outlining genome-wide metabolic networks in *Burkholderia xenovorans* LB400. Appl Environ Microbiol. 2004;70(8):4961-70.
11. Denef VJ, Klappenbach JA, Patrauchan MA, Florizone C, Rodrigues JL, Tsoi TV, Verstraete W, Eltis LD, Tiedje JM. Genetic and genomic insights into the role of benzoate-catabolic pathway redundancy in *Burkholderia xenovorans* LB400. Appl Environ Microbiol. 2006;72(1):585-95.
12. Parnell JJ, Park J, Denef V, Tsoi T, Hashsham S, Quensen J, 3rd, Tiedje JM. Coping with polychlorinated biphenyl (PCB) toxicity: Physiological and genome-wide responses of *Burkholderia xenovorans* LB400 to PCB-mediated stress. Appl Environ Microbiol. 2006;72(10):6607-14.
13. Patrauchan MA, Parnell JJ, McLeod MP, Florizone C, Tiedje JM, Eltis LD. Genomic analysis of the phenylacetyl-CoA pathway in *Burkholderia xenovorans* LB400. Arch Microbiol. 2011;193(9):641-50.
14. Miyakoshi M, Shintani M, Terabayashi T, Kai S, Yamane H, Nojiri H. Transcriptome analysis of *Pseudomonas putida* KT2440 harboring the completely sequenced IncP-7 plasmid pCAR1. J Bacteriol. 2007;189(19):6849-60.
15. Wang Y, Morimoto S, Ogawa N, Fujii T. A survey of the cellular responses in *Pseudomonas putida* KT2440 growing in sterilized soil by microarray analysis. FEMS Microbiol Ecol. 2011;78(2):220-32.
16. Miyazaki R, Yano H, Sentchilo V, van der Meer JR. Physiological and transcriptome changes induced by *Pseudomonas putida* acquisition of an integrative and conjugative element. Sci Rep. 2018;8(1):5550.
17. Puglisi E, Cahill MJ, Lessard PA, Capri E, Sinskey AJ, Archer JA, Boccazzi P. Transcriptional response of *Rhodococcus aetherivorans* I24 to polychlorinated biphenyl-contaminated sediments. Microb Ecol. 2010;60(3):505-15.
18. Gonçalves ER, Hara H, Miyazawa D, Davies JE, Eltis LD, Mohn WW. Transcriptomic assessment of isozymes in the biphenyl pathway of *Rhodococcus* sp. strain RHA1. Appl Environ Microbiol. 2006;72(9):6183-93.
19. Hara H, Eltis LD, Davies JE, Mohn WW. Transcriptomic analysis reveals a bifurcated terephthalate degradation pathway in *Rhodococcus* sp. strain RHA1. J Bacteriol. 2007;189(5):1641-7.
20. Iino T, Wang Y, Miyauchi K, Kasai D, Masai E, Fujii T, Ogawa N, Fukuda M. Specific gene responses of *Rhodococcus jostii* RHA1 during growth in soil. Appl Environ Microbiol. 2012;78(19):6954-62.
21. Imperlini E, Bianco C, Lonardo E, Camerini S, Cermola M, Moschetti G, Defez R. Effects of indole-3-acetic acid on *Sinorhizobium meliloti* survival and on symbiotic nitrogen fixation and stem dry weight production. Appl Microbiol Biotechnol. 2009;83(4):727-38.
22. Flood JJ, Copley SD. Genome-wide analysis of transcriptional changes and genes that contribute to fitness during degradation of the anthropogenic pollutant pentachlorophenol by *Sphingobium chlorophenolicum*. mSystems. 2018;3(6).
23. Pérez-Pantoja D, Leiva-Novoa P, Donoso RA, Little C, Godoy M, Pieper DH, González B. Hierarchy of carbon source utilization in soil bacteria: Hegemonic preference for benzoate in complex aromatic compound mixtures degraded by *Cupriavidus pinatubonensis* strain JMP134. Appl Environ Microbiol. 2015;81(12):3914-24.
24. Fang L, Shi T, Chen Y, Wu X, Zhang C, Tang X, Li QX, Hua R. Kinetics and catabolic pathways of the insecticide chlorpyrifos, annotation of the degradation genes, and characterization of enzymes TcpA and Fre in *Cupriavidus nantongensis* X1^{T}. J Agric Food Chem. 2019;67(8):2245-54.
25. Xiang S, Lin R, Shang H, Xu Y, Zhang Z, Wu X, Zong F. Efficient degradation of phenoxyalkanoic acid herbicides by the alkali-tolerant *Cupriavidus oxalaticus* strain X32. J Agric Food Chem. 2020;68(12):3786-95.

26. Ogawa N, Miyashita K. Recombination of a 3-chlorobenzoate catabolic plasmid from *Alcaligenes eutrophus* NH9 mediated by direct repeat elements. Appl Environ Microbiol. 1995;61(11):3788-95.
27. Moriuchi R, Dohra H, Kanesaki Y, Ogawa N. Complete genome sequence of 3-chlorobenzoate-degrading bacterium *Cupriavidus necator* NH9 and reclassification of the strains of the genera *Cupriavidus* and *Ralstonia* based on phylogenetic and whole-genome sequence analyses. Front Microbiol. 2019;10:133.
28. Ogawa N, McFall SM, Klem TJ, Miyashita K, Chakrabarty AM. Transcriptional activation of the chlorocatechol degradative genes of *Ralstonia eutropha* NH9. J Bacteriol. 1999;181(21):6697-705.
29. Bott TL, Kaplan LA. Autecological properties of 3-chlorobenzoate-degrading bacteria and their population dynamics when introduced into sediments. Microb Ecol. 2002;43(2):199-216.
30. Gibson J, C SH. Metabolic diversity in aromatic compound utilization by anaerobic microbes. Annu Rev Microbiol. 2002;56:345-69.
31. Ogawa N, Miyashita K, Chakrabarty AM. Microbial genes and enzymes in the degradation of chlorinated compounds. Chem Rec. 2003;3(3):158-71.
32. Ogawa N, Miyashita K. The chlorocatechol-catabolic transposon Tn*5707* of *Alcaligenes eutrophus* NH9, carrying a gene cluster highly homologous to that in the 1,2,4-trichlorobenzene-degrading bacterium *Pseudomonas* sp. strain P51, confers the ability to grow on 3-chlorobenzoate. Appl Environ Microbiol. 1999;65(2):724-31.
33. Ismail W, Gescher J. Epoxy coenzyme A thioester pathways for degradation of aromatic compounds. Appl Environ Microbiol. 2012;78(15):5043-51.
34. Chang HK, Mohseni P, Zylstra GJ. Characterization and regulation of the genes for a novel anthranilate 1,2-dioxygenase from *Burkholderia cepacia* DBO1. J Bacteriol. 2003;185(19):5871-81.
35. Ledger T, Aceituno F, Gonzalez B. 3-chlorobenzoate is taken up by a chromosomally encoded transport system in *Cupriavidus necator* JMP134. Microbiology. 2009;155(Pt 8):2757-65.
36. Xu Y, Gao X, Wang SH, Liu H, Williams PA, Zhou NY. MhbT is a specific transporter for 3-hydroxybenzoate uptake by Gram-negative bacteria. Appl Environ Microbiol. 2012;78(17):6113-20.
37. Harwood CS, Nichols NN, Kim MK, Ditty JL, Parales RE. Identification of the *pcaRKF* gene cluster from *Pseudomonas putida*: involvement in chemotaxis, biodegradation, and transport of 4-hydroxybenzoate. J Bacteriol. 1994;176(21):6479-88.
38. Nichols NN, Harwood CS. PcaK, a high-affinity permease for the aromatic compounds 4-hydroxybenzoate and protocatechuate from *Pseudomonas putida*. J Bacteriol. 1997;179(16):5056-61.
39. MacLean AM, Haerty W, Golding GB, Finan TM. The LysR-type PcaQ protein regulates expression of a protocatechuate-inducible ABC-type transport system in *Sinorhizobium meliloti*. Microbiology. 2011;157(Pt 9):2522-33.
40. Reva ON, Weinel C, Weinel M, Böhm K, Stjepandic D, Hoheisel JD, Tümmler B. Functional genomics of stress response in *Pseudomonas putida* KT2440. J Bacteriol. 2006;188(11):4079-92.
41. Parales RE, Luu RA, Hughes JG, Ditty JL. Bacterial chemotaxis to xenobiotic chemicals and naturally-occurring analogs. Curr Opin Biotechnol. 2015;33:318-26.
42. Bi S, Sourjik V. Stimulus sensing and signal processing in bacterial chemotaxis. Curr Opin Microbiol. 2018;45:22-9.
43. Chen GQ. A microbial polyhydroxyalkanoates (PHA) based bio- and materials industry. Chem Soc Rev. 2009;38(8):2434-46.
44. Peoples OP, Sinskey AJ. Poly-beta-hydroxybutyrate biosynthesis in *Alcaligenes eutrophus* H16. Characterization of the genes encoding beta-ketothiolase and acetoacetyl-CoA reductase. J Biol Chem. 1989;264(26):15293-7.
45. Kutralam-Muniasamy G, Peréz-Guevara F. Genome characteristics dictate poly-R-(3)-hydroxyalkanoate production in *Cupriavidus necator* H16. World J Microbiol Biotechnol. 2018;34(6):79.
46. Lin LX, Liu H, Zhou NY. MhbR, a LysR-type regulator involved in 3-hydroxybenzoate catabolism via gentisate in *Klebsiella pneumoniae* M5a1. Microbiol Res. 2010;165(1):66-74.
47. Olivera ER, Miñambres B, García B, Muñiz C, Moreno MA, Ferrández A, Díaz E, García JL, Luengo JM. Molecular characterization of the phenylacetic acid catabolic pathway in *Pseudomonas putida* U: the phenylacetyl-CoA catabolon. Proc Natl Acad Sci USA. 1998;95(11):6419-24.
48. Chae JC, Zylstra GJ. 4-chlorobenzoate uptake in *Comamonas* sp. strain DJ-12 is mediated by a tripartite ATP-independent periplasmic transporter. J Bacteriol. 2006;188(24):8407-12.
49. Hosaka M, Kamimura N, Toribami S, Mori K, Kasai D, Fukuda M, Masai E. Novel tripartite aromatic acid transporter essential for terephthalate uptake in *Comamonas* sp. strain E6. Appl Environ Microbiol. 2013;79(19):6148-55.
50. Reverón I, Jiménez N, Curiel JA, Peñas E, López de Felipe F, de Las Rivas B, Muñoz R. Differential gene expression by *Lactobacillus plantarum* WCFS1 in response to phenolic compounds reveals new genes involved in tannin degradation. Appl Environ Microbiol.

2017;83(7).

51. Gaucher F, Bonnassie S, Rabah H, Marchand P, Blanc P, Jeantet R, Jan G. Review: Adaptation of beneficial propionibacteria, lactobacilli, and bifidobacteria improves tolerance toward technological and digestive stresses. Front Microbiol. 2019;10:841.
52. Lundgren CAK, Sjöstrand D, Biner O, Bennett M, Rudling A, Johansson AL, Brzezinski P, Carlsson J, von Ballmoos C, Högbom M. Scavenging of superoxide by a membrane-bound superoxide oxidase. Nat Chem Biol. 2018;14(8):788-93.
53. Tamburro A, Robuffo I, Heipieper HJ, Allocati N, Rotilio D, Di Ilio C, Favaloro B. Expression of glutathione S-transferase and peptide methionine sulphoxide reductase in *Ochrobactrum anthropi* is correlated to the production of reactive oxygen species caused by aromatic substrates. FEMS Microbiol Lett 2004;241(2):151-6.
54. Chávez FP, Lünsdorf H, Jerez CA. Growth of polychlorinated-biphenyl-degrading bacteria in the presence of biphenyl and chlorobiphenyls generates oxidative stress and massive accumulation of inorganic polyphosphate. Appl Environ Microbiol. 2004;70(5):3064-72.
55. Mason JR, Cammack R. The electron-transport proteins of hydroxylating bacterial dioxygenases. Annu Rev Microbiol. 1992;46:277-305.
56. Welch M, Oosawa K, Aizawa S, Eisenbach M. Phosphorylation-dependent binding of a signal molecule to the flagellar switch of bacteria. Proc Natl Acad Sci USA. 1993;90(19):8787-91.
57. Sarkar MK, Paul K, Blair D. Chemotaxis signaling protein CheY binds to the rotor protein FliN to control the direction of flagellar rotation in *Escherichia coli*. Proc Natl Acad Sci USA. 2010;107(20):9370-5.
58. Nishikino T, Hijikata A, Miyanoiri Y, Onoue Y, Kojima S, Shirai T, Homma M. Rotational direction of flagellar motor from the conformation of FliG middle domain in marine *Vibrio*. Sci Rep. 2018;8(1):17793.
59. Leveau JH, Zehnder AJ, van der Meer JR. The *tfdK* gene product facilitates uptake of 2,4-dichlorophenoxyacetate by *Ralstonia eutropha* JMP134(pJP4). J Bacteriol. 1998;180(8):2237-43.
60. Hawkins AC, Harwood CS. Chemotaxis of *Ralstonia eutropha* JMP134(pJP4) to the herbicide 2,4-dichlorophenoxyacetate. Appl Environ Microbiol. 2002;68(2):968-72.
61. Reams AB, Neidle EL. Selection for gene clustering by tandem duplication. Annu Rev Microbiol. 2004;58:119-42.
62. Luu RA, Kootstra JD, Nesteryuk V, Brunton CN, Parales JV, Ditty JL, Parales RE. Integration of chemotaxis, transport and catabolism in *Pseudomonas putida* and identification of the aromatic acid chemoreceptor PcaY. Mol Microbiol. 2015;96(1):134-47.
63. Collier LS, Nichols NN, Neidle EL. *benK* encodes a hydrophobic permease-like protein involved in benzoate degradation by *Acinetobacter* sp. strain ADP1. J Bacteriol. 1997;179(18):5943-6.
64. Bolger AM, Lohse M, Usadel B. Trimmomatic: a flexible trimmer for Illumina sequence data. Bioinformatics. 2014;30(15):2114-20.
65. Kim D, Langmead B, Salzberg SL. HISAT: a fast spliced aligner with low memory requirements. Nat Methods. 2015;12(4):357-60.
66. Pertea M, Pertea GM, Antonescu CM, Chang TC, Mendell JT, Salzberg SL. StringTie enables improved reconstruction of a transcriptome from RNA-seq reads. Nat Biotechnol. 2015;33(3):290-5.
67. Robinson MD, McCarthy DJ, Smyth GK. edgeR: a Bioconductor package for differential expression analysis of digital gene expression data. Bioinformatics. 2010;26(1):139-40.
68. Mitchell A, Chang HY, Daugherty L, Fraser M, Hunter S, Lopez R, McAnulla C, McMenamin C, Nuka G, Pesseat S, Sangrador-Vegas A, Scheremetjew M, Rato C, Yong SY, Bateman A, Punta M, Attwood TK, Sigrist CJ, Redaschi N, Rivoire C, Xenarios I, Kahn D, Guyot D, Bork P, Letunic I, Gough J, Oates M, Haft D, Huang H, Natale DA, Wu CH, Orengo C, Sillitoe I, Mi H, Thomas PD, Finn RD. The InterPro protein families database: the classification resource after 15 years. Nucleic Acids Res. 2015;43(Database issue):D213-21.
69. Ashburner M, Ball CA, Blake JA, Botstein D, Butler H, Cherry JM, Davis AP, Dolinski K, Dwight SS, Eppig JT, Harris MA, Hill DP, Issel-Tarver L, Kasarskis A, Lewis S, Matese JC, Richardson JE, Ringwald M, Rubin GM, Sherlock G. Gene ontology: tool for the unification of biology. The Gene Ontology Consortium. Nat Genet. 2000;25(1):25-9.
70. Kim SY, Volsky DJ. PAGE: parametric analysis of gene set enrichment. BMC Bioinformatics. 2005;6:144.
71. Yamamoto-Tamura K, Kawagishi I, Ogawa N, Fujii T. A putative porin gene of *Burkholderia* sp. NK8 involved in chemotaxis toward β-ketoadipate. Biosci Biotechnol Biochem. 2015;79(6):926-36.
72. Kumar S, Stecher G, Tamura K. MEGA7: Molecular Evolutionary Genetics Analysis Version 7.0 for Bigger Datasets. Mol Biol Evol. 2016;33(7):1870-4.
73. Saitou N, Nei M. The neighbor-joining method: a new method for reconstructing phylogenetic trees. Mol Biol Evol. 1987;4(4):406-25.

Tables

Table 1 Expression of genes involved in degradation of 3-chlorobenzoate and benzoate in NH9

Compound	Replicon	Locus	Gene[a]	K number	Definition[a]	3-CB vs. CA		BA vs. CA		3-CB vs. BA	
						LogFC[b,c]	FDR[d]	LogFC[b,e]	FDR[d]	LogFC[b,f]	FDR[d]
3-Chlorobenzoate and Benzoate	Chr.1	BJN34_08560	*benA*	K05549	Benzoate 1,2-dioxygenase alpha subunit	8.2	1.2E-80	8.1	5.6E-79	0.092	9.0E-01
		BJN34_08565	*benB*	K05550	Benzoate 1,2-dioxygenase beta subunit	8.2	1.2E-91	8.0	5.1E-88	0.20	7.2E-01
		BJN34_08570	*benC*	K05784	Benzoate 1,2-dioxygenase reductase component	8.5	6.1E-140	8.3	4.9E-135	0.19	6.7E-01
		BJN34_08575	*benD*	K05783	1,6-Dihydroxycyclohexa-2,4-diene-1-carboxylate dehydrogenase	8.4	1.7E-117	8.4	4.4E-118	-0.048	9.4E-01
Benzoate	Chr.1	BJN34_07180	*boxA*	K15511	Benzoyl-CoA 2,3-epoxidase subunit A	1.3	2.8E-04	3.5	1.1E-25	-2.2	2.9E-12
		BJN34_07185	*boxB*	K15512	Benzoyl-CoA 2,3-epoxidase subunit B	1.1	9.9E-03	4.0	1.9E-23	-2.9	2.9E-14
		BJN34_07190	*boxC*	K15513	Benzoyl-CoA-dihydrodiol lyase	0.0052	9.9E-01	2.4	2.5E-05	-2.4	2.3E-05
		BJN34_07200	*bclA*	K04110	Benzoate-CoA ligase	0.67	4.8E-01	1.8	5.2E-02	-1.2	2.8E-01
	Chr.2	BJN34_32090	*boxA*	K15511	Benzoyl-CoA 2,3-epoxidase subunit A	0.56	3.3E-01	4.0	4.2E-23	-3.5	1.1E-19
		BJN34_32095	*boxB*	K15512	Benzoyl-CoA 2,3-epoxidase subunit B	0.51	3.5E-01	4.4	5.2E-24	-3.8	1.8E-20
		BJN34_32100	*boxC*	K15513	Benzoyl-CoA-dihydrodiol lyase	0.49	4.5E-01	3.8	3.2E-13	-3.3	6.5E-11
		BJN34_32115	*boxD*	K15514	3,4-Dehydroadipyl-CoA semialdehyde dehydrogenase	0.20	8.3E-01	4.9	6.9E-16	-4.7	2.0E-15
3-Chlorocatechol	pENH91	BJN34_37380	*cbnA*	K15253	Chlorocatechol 1,2-dioxygenase	9.9	7.5E-151	1.3	2.5E-05	8.6	2.5E-126
		BJN34_37385	*cbnB*	K01860	Chloromuconate cycloisomerase	9.8	2.2E-90	1.5	3.4E-04	8.3	2.0E-73
		BJN34_37395	*cbnC*	K01061	Dienelactone hydrolase	9.5	7.4E-148	1.4	3.1E-05	8.2	2.2E-123
		BJN34_37400	*cbnD*	K00217	Maleylacetate reductase	9.4	1.7E-122	1.5	2.9E-05	7.9	8.9E-100
Catechol	Chr.1	BJN34_08555	*catA*	K03381	Catechol 1,2-dioxygenase	6.0	5.8E-77	6.2	9.8E-80	-0.18	7.3E-01
	Chr.2	BJN34_24340	*catB*	K01856	Muconate cycloisomerase	5.6	2.9E-15	6.7	1.1E-19	-1.2	1.7E-01
		BJN34_29740	*catC*	K01055	3-Oxoadipate enol-lactonase	6.0	1.7E-67	6.0	8.8E-68	-0.044	9.5E-01
		BJN34_29745	*catD*	K03464	Muconolactone isomerase	5.9	7.7E-54	6.0	1.7E-54	-0.077	9.1E-01
3-Oxoadipate	Chr.2	BJN34_21015	*pcaI*	K01031	3-Oxoadipate CoA-transferase alpha subunit	4.5	2.9E-23	4.7	3.8E-24	-0.14	8.6E-01
		BJN34_21020	*pcaJ*	K01032	3-Oxoadipate CoA-transferase beta subunit	5.5	1.9E-28	5.3	2.7E-26	0.24	7.6E-01
		BJN34_21025	*pcaF*	K00632	3-Oxoadipyl-CoA thiolase	5.9	1.8E-41	5.4	3.3E-36	0.48	4.1E-01

[a]Gene designations and definitions from KEGG annotation were manually modified.

[b]LogFC indicates log fold-change.

[c]LogFC calculated from 3-CB/CA.

[d]FDR indicates false discovery rate.

[e]LogFC calculated from BA/CA.

[f]LogFC calculated from 3-CB/BA.

Table 2 Significantly expressed genes encoding MFS and ABC transporters in NH9

Family	Replicon	Locus	Component[a]	K number	Protein	Accession number	%Amino acid identity	3-CB vs. CA		BA vs. CA		3-CB vs. BA	
								LogFC[b, c]	FDR[d]	LogFC[b, e]	FDR[d]	LogFC[b, f]	FDR[d]
Major facilitator superfamily (MFS)													
Aromatic acid:H^+ symporter (AAHS) family													
	Chr.1	BJN34_18155	-	K05548	BenP	AAZ63295.1	70.4	3.1	3.4E-20	0.12	8.9E-01	2.9	4.9E-20
	Chr.2	BJN34_30890	-	K08195	MhbT	AAW63412.1	52.1	4.2	1.3E-20	0.019	9.9E-01	4.1	2.6E-21
		BJN34_32125	-	K05548	BenP	AAZ63295.1	77.2	0.14	8.6E-01	4.5	4.4E-24	-4.3	3.8E-24
		BJN34_33870	-	K08195	PcaK	AAA85137.1	55.1	2.9	8.7E-09	1.3	2.0E-02	1.5	6.5E-03
Drug:H^+ antiporter-2 (14 spanner) (DHA2) family													
	Chr.1	BJN34_11715	-	K03446	PcaK	CAG68551.1	25.8	2.0	2.2E-07	1.8	1.5E-05	0.24	7.2E-01
		BJN34_12320	-	K19577	MhpT	APC50650.1	29.3	2.1	6.4E-11	-0.064	9.3E-01	2.1	1.3E-11
Metabolite:H^+ symporter (MHS) family													
	Chr.2	BJN34_20520	-	K03761	MopB	AAB41509.1	31.5	2.7	2.5E-10	2.1	1.7E-06	0.57	3.4E-01
Cyanate porter (CP) family													
	Chr.2	BJN34_26825	-	K03449	HpaX	ADT77978.1	26.8	2.9	1.4E-06	3.2	1.6E-07	-0.36	7.2E-01
ATP-binding cassette (ABC)													
Branched-chain amino acid transporter													
	Chr.1	BJN34_01710	NBD	K01995	HmgG	AAY18213.1	40.0	2.8	1.2E-11	2.1	5.0E-06	0.74	1.2E-01
		BJN34_01715	TMD	K01997	HmgE	AAY18215.1	28.3	2.7	5.5E-04	2.2	1.2E-02	0.46	6.9E-01
		BJN34_01720	TMD	K01998	HmgF	AAY18214.1	31.4	1.9	2.9E-05	1.5	4.3E-03	0.40	5.2E-01
		BJN34_01725	SBP	K01999	-	-	-	1.9	9.6E-09	1.4	1.5E-04	0.53	2.3E-01
		BJN34_01730	NBD	K01996	HmgH	AAY18212.1	44.3	2.1	3.0E-04	1.6	1.8E-02	0.49	5.6E-01
		BJN34_07675	SBP	K01999	-	-	-	1.8	1.2E-05	2.0	3.9E-06	-0.17	8.3E-01
		BJN34_07680	TMD	K01997	HmgE	AAY18215.1	24.6	0.51	3.2E-01	1.3	1.1E-02	-0.75	1.9E-01
		BJN34_07685	TMD	K01998	PcaV	CAC49878.1	24.9	0.91	4.9E-02	1.4	3.9E-03	-0.48	4.6E-01
		BJN34_07690	NBD	K01995	PcaW	CAC49877.1	34.3	0.062	9.7E-01	3.6	1.4E-03	-3.5	2.0E-03
		BJN34_07695	NBD	K01996	HmgH	AAY18212.1	40.7	1.0	2.4E-02	0.98	5.9E-02	0.030	9.8E-01
		BJN34_11495	TMD	K01998	PcaV	CAC49878.1	30.6	2.7	4.2E-13	2.1	7.3E-08	0.63	2.0E-01
		BJN34_11500	TMD	K01997	HmgE	AAY18215.1	29.5	3.0	9.7E-15	2.3	7.7E-09	0.72	1.6E-01
		BJN34_11505	NBD	K01996	HmgH	AAY18212.1	37.4	3.0	2.9E-18	2.4	2.4E-11	0.66	1.3E-01
		BJN34_11510	NBD	K01995	PcaW	CAC49877.1	40.2	0.72	3.6E-01	0.39	7.6E-01	0.34	7.7E-01
		BJN34_11515	SBP	K01999	PcaM	CAC49880.1	23.5	3.2	1.7E-17	2.3	1.5E-09	0.90	5.0E-02
	Chr.2	BJN34_29445	SBP	K01999	PcaM	CAC49880.1	27.7	9.4	1.0E-89	1.5	3.8E-02	7.9	6.9E-80
		BJN34_29450	NBD	K01995	PcaW	CAC49877.1	35.8	11.0	2.3E-85	3.8	1.4E-05	7.3	1.8E-67
		BJN34_29455	NBD	K01996	PcaX	CAC49876.1	40.3	8.9	5.3E-91	0.91	3.8E-01	8.0	4.4E-88
		BJN34_29460	TMD	K01997	PcaN	CAC49879.1	33.3	8.1	3.8E-05	1.5	5.6E-01	6.6	1.1E-03
		BJN34_29465	TMD	K01998	PcaV	CAC49878.1	32.4	7.7	2.5E-27	0.47	7.3E-01	7.2	8.9E-26
		BJN34_32550	TMD	K01997	HmgE	AAY18215.1	38.5	0.56	2.3E-01	0.55	3.4E-01	0.0051	1.0E+00
		BJN34_32555	TMD	K01998	HmgF	AAY18214.1	27.3	2.5	5.4E-06	2.2	2.7E-04	0.30	7.0E-01
		BJN34_32560	NBD	K01995	HmgG	AAY18213.1	41.9	1.3	1.4E-02	1.5	4.6E-03	-0.27	7.2E-01
		BJN34_32565	NBD	K01996	HmgH	AAY18212.1	45.5	2.5	1.0E-04	2.2	2.2E-03	0.29	7.4E-01
		BJN34_32570	SBP	K01999	HmgD	AAY18216.1	28.4	1.6	1.1E-	1.0	7.0E-	0.57	1.8E-01

								06		03		
NitT/TauT family transporter												
Chr.1	BJN34_09335	SBP	K02051	-	-	-	1.3	2.9E-02	0.40	7.0E-01	0.89	2.3E-01
	BJN34_09340	NBD	K02049	PatA	ABG99217.1	41.4	2.3	5.1E-06	0.82	3.4E-01	1.5	3.1E-03
	BJN34_09345	TMD	K02050	PatC	ABG99215.1	27.0	2.2	8.8E-04	1.2	2.0E-01	1.0	1.9E-01
pENH92	BJN34_36080	SBP	K02051	-	-	-	1.2	1.9E-01	-1.2	3.9E-01	2.4	2.5E-02
	BJN34_36095	TMD	K02050	PatB	ABG99216.1	26.9	2.5	4.6E-04	-0.018	9.9E-01	2.5	7.9E-04
	BJN34_36100	NBD	K02049	PatA	ABG99217.1	44.1	2.9	3.5E-04	1.8	1.2E-01	1.2	1.8E-01
Glycerol transporter												
Chr.1	BJN34_13400	SBP	K17321	-	-	-	2.3	4.3E-09	1.4	2.3E-03	0.97	4.3E-02
	BJN34_13410	TMD	K17323	-	-	-	2.0	2.3E-05	1.6	2.2E-03	0.35	5.8E-01
	BJN34_13415	TMD	K17322	-	-	-	1.6	1.5E-03	1.6	3.3E-03	-0.0088	9.9E-01
	BJN34_13420	NBD	K17325	OphH	BAG45601.1	34.9	2.2	1.3E-02	1.4	1.9E-01	0.74	5.7E-01
	BJN34_13425	NBD	K17324	PatA	ABG99217.1	30.3	1.2	7.3E-04	1.1	6.2E-03	0.11	8.6E-01
Putative polar amino acid transporter												
Chr.1	BJN34_14830	TMD	K02029	-	-	-	2.7	4.9E-07	-0.40	7.2E-01	3.1	1.5E-08
	BJN34_14835	TMD	K02029	-	-	-	3.7	1.1E-05	1.2	3.1E-01	2.5	5.4E-03
	BJN34_14840	NBD	K02028	OphH	BAG45601.1	35.3	2.7	1.6E-10	1.1	5.6E-02	1.7	1.1E-04
	BJN34_14845	SBP	K02030	-	-	-	2.0	9.1E-07	0.70	2.2E-01	1.3	3.7E-03
ABC-2 type transporter												
Chr.2	BJN34_25255	NBD	K01990	OphH	BAG45601.1	31.9	3.5	1.7E-02	2.3	2.5E-01	1.1	4.9E-01
	BJN34_25270	TMD	K01992	-	-	-	4.8	1.2E-02	4.7	3.5E-02	0.14	9.5E-01
Ribose transporter												
Chr.2	BJN34_29355	NBD	K10441	HmgG	AAY18213.1	28.3	2.6	1.3E-11	2.0	6.6E-07	0.61	2.4E-01
	BJN34_29360	TMD	K10440	HmgE	AAY18215.1	26.0	2.6	2.6E-08	2.4	5.0E-07	0.17	8.4E-01
	BJN34_29365	SBP	K10439	-	-	-	2.5	6.2E-10	2.6	3.0E-10	-0.077	9.2E-01
Other ABC transporters												
Chr.1	BJN34_11055	NBD, TMD	K02471	HmgG	AAY18213.1	38.0	2.4	1.1E-02	1.6	2.0E-01	0.85	5.2E-01

[a]NBD, nucleotide binding domain; SBP, substrate binding protein; TMD, transmembrane domain.
[b]LogFC indicates log fold-change.
[c]LogFC calculated from 3-CB/CA.
[d]FDR indicates false discovery rate.
[e]LogFC calculated from BA/CA.
[f]LogFC calculated from 3-CB/BA.

Figures

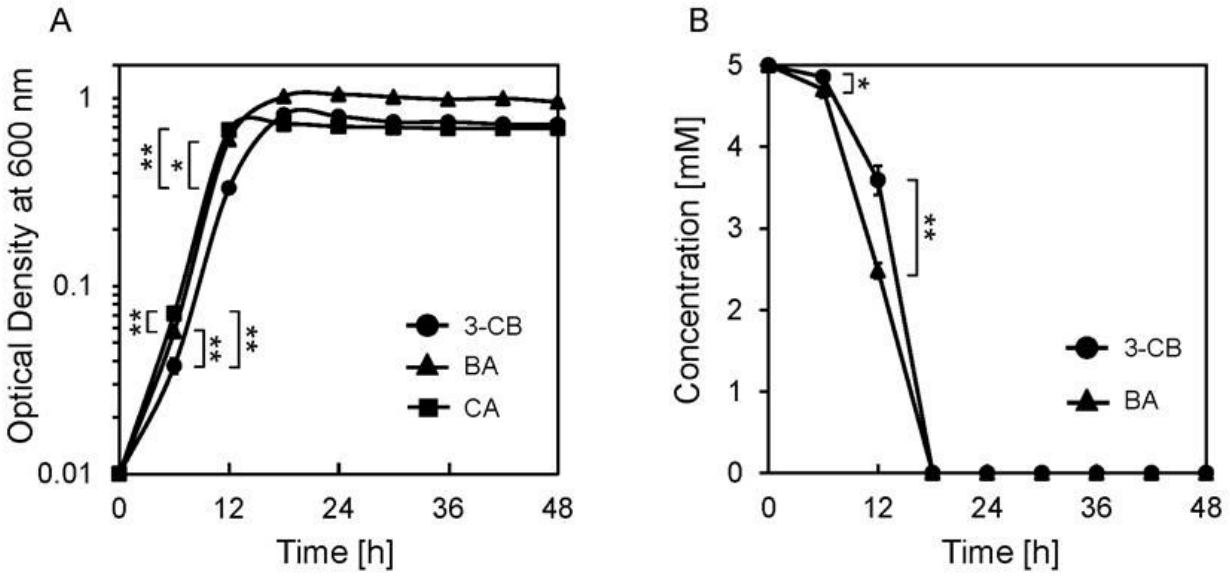

Figure 1

Growth curves and aromatic compound degradation abilities of C. necator NH9. Time course of bacterial growth (A) and aromatic compound degradation (B) of strain NH9. Cells were grown on basal salts medium supplemented with 5 mM 3-chlorobenzoate (circles), benzoate (triangles), or citric acid (squares). Data are averages ± standard deviations of three independent experiments. * and ** indicate significant differences at $p < 0.05$ and $p < 0.01$, respectively (paired t-test). There was no significant difference in optical density at 600 nm (OD600) values between benzoate and citric acid samples at 12 h.

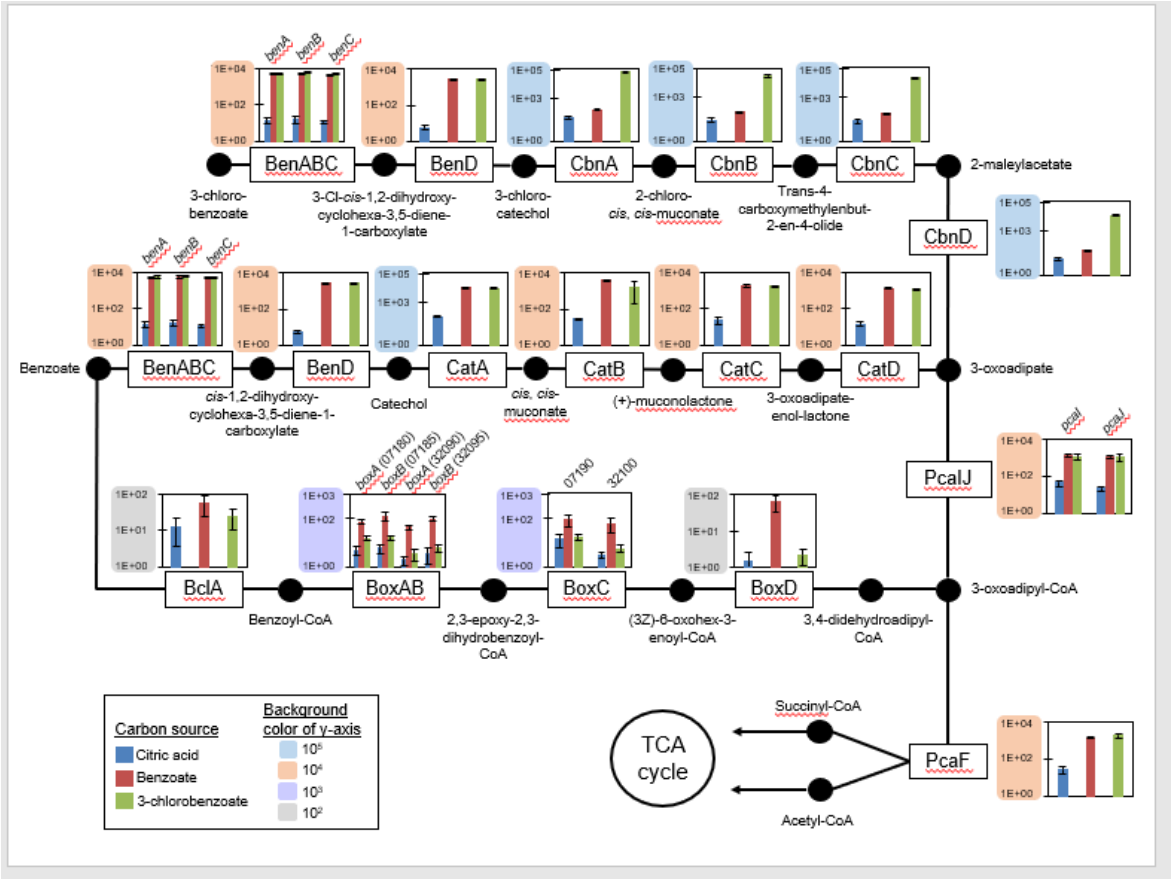

Figure 2

Transcript levels of genes involved in degradation of 3-chlorobenzoate and benzoate. Boxes and black circles indicate enzymes and compounds, respectively. Transcripts per million (TPM) values of each gene are average of triplicates and are shown in bar graphs. Scales of vertical axes of graph are categorized into four groups with the following colors: blue, 105; orange, 104; purple, 103; and gray, 102.

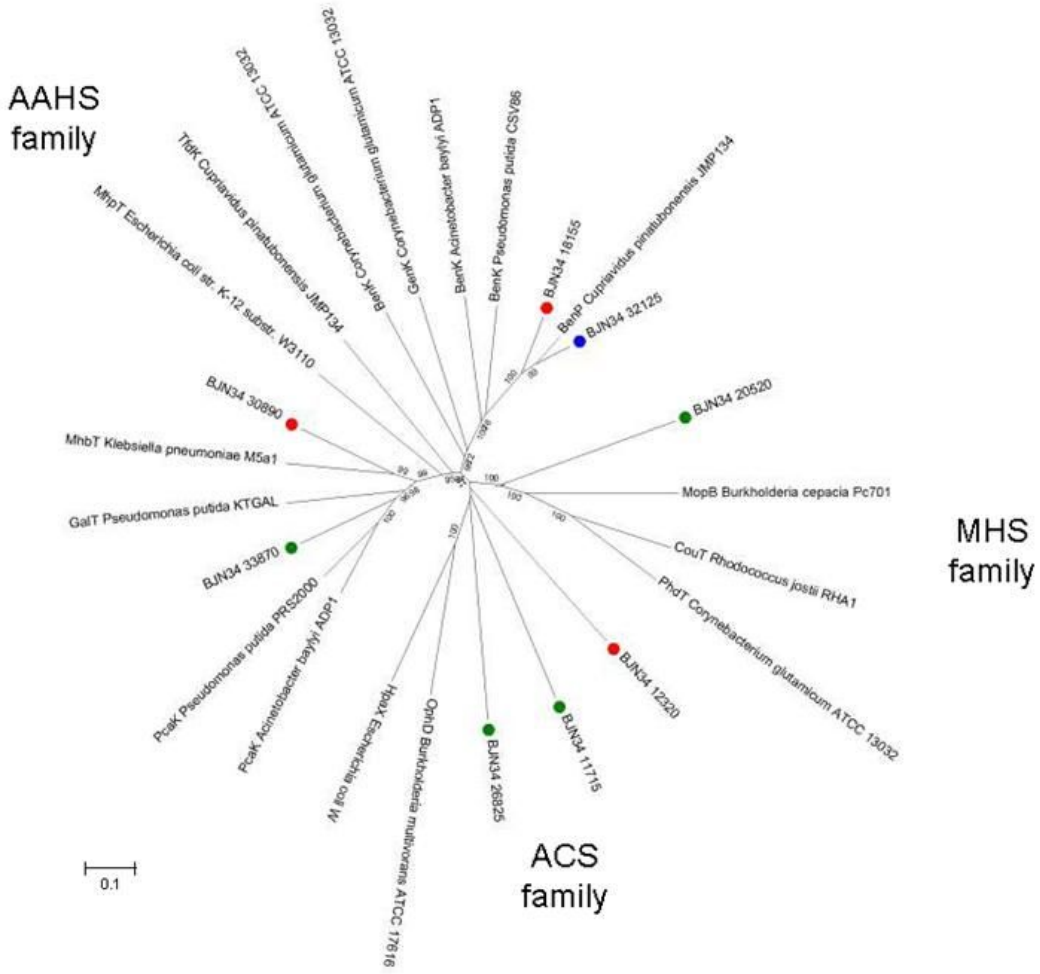

Figure 3

Evolutionary relationships among MFS transporters. Construction of evolutionary tree and ClustalW alignments were performed with MEGA version 7.0 [72]. Evolutionary relationships were inferred using the neighbor-joining method [73]. Red, blue, and green circles mark genes encoding major facilitator superfamily (MFS) transporters in NH9 expressed specifically in response to 3-chlorobenzoate, benzoate, and both compounds, respectively. Aromatic acid:H+ symporter (AAHS) family includes BenK from Acinetobacter baylyi ADP1, BenK from Corynebacterium glutamicum ATCC 13032, BenK from Pseudomonas putida CSV86, BenP from Cupriavidus pinatubonensis JMP134, GalT from Pseudomonas putida KTGAL, GenK from C. glutamicum ATCC 13032, MhbT from Klebsiella pneumoniae M5a1, MhpT from Escherichia coli K-12 substr. W3110, PcaK from A. baylyi ADP1, PcaK from Pseudomonas putida PRS2000, and TfdK from C. pinatubonensis JMP134. Anion/cation symporter (ACS) family includes HpaX from Escherichia coli W and OphD from Burkholderia multivorans ATCC 17616. Metabolite:H+ symporter (MHS) family includes CouT from Rhodococcus jostii RHA1, MopB from Burkholderia cepacia Pc701, and PhdT from C. glutamicum ATCC 13032. See Table S5 for detailed information about proteins.

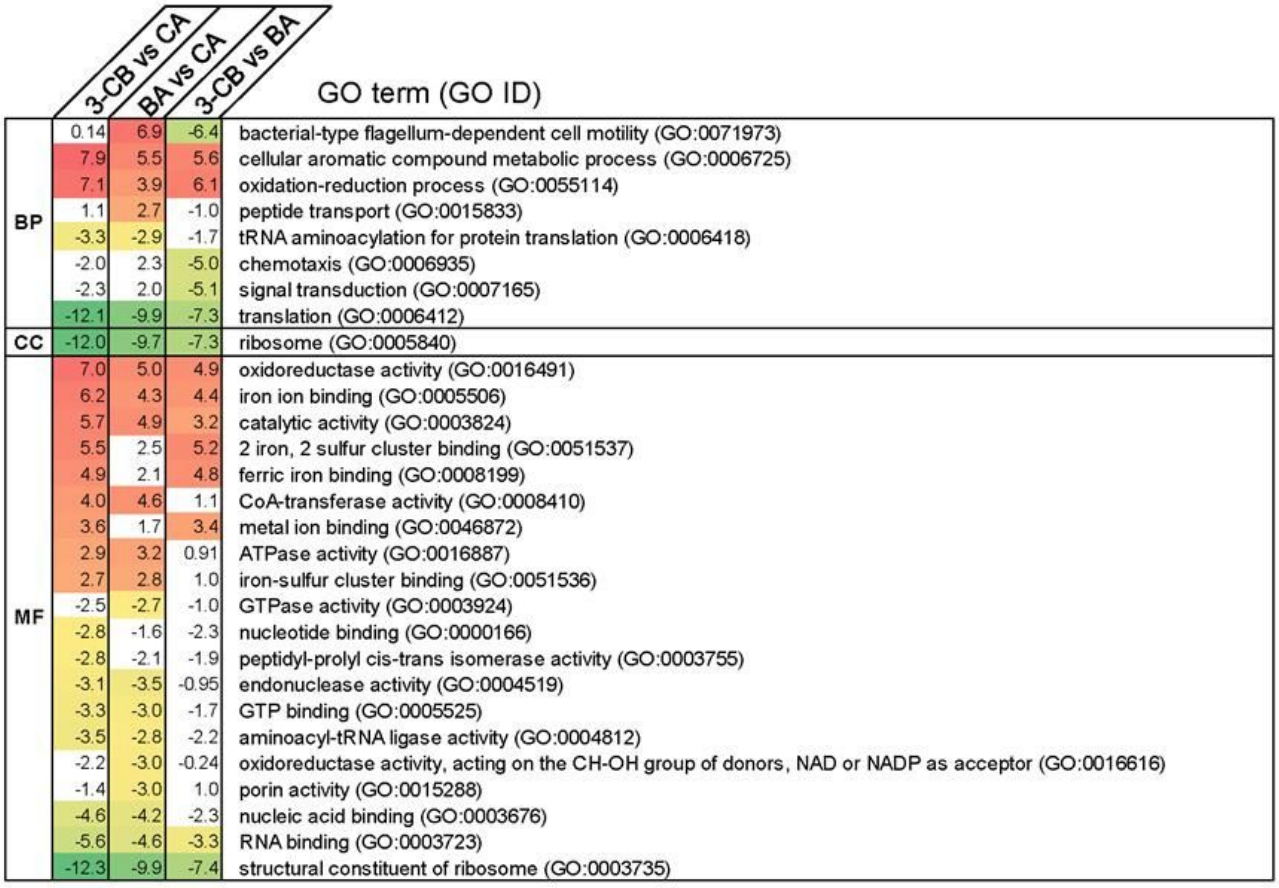

	3-CB vs CA	BA vs CA	3-CB vs BA	GO term (GO ID)
BP	0.14	6.9	-6.4	bacterial-type flagellum-dependent cell motility (GO:0071973)
	7.9	5.5	5.6	cellular aromatic compound metabolic process (GO:0006725)
	7.1	3.9	6.1	oxidation-reduction process (GO:0055114)
	1.1	2.7	-1.0	peptide transport (GO:0015833)
	-3.3	-2.9	-1.7	tRNA aminoacylation for protein translation (GO:0006418)
	-2.0	2.3	-5.0	chemotaxis (GO:0006935)
	-2.3	2.0	-5.1	signal transduction (GO:0007165)
	-12.1	-9.9	-7.3	translation (GO:0006412)
CC	-12.0	-9.7	-7.3	ribosome (GO:0005840)
MF	7.0	5.0	4.9	oxidoreductase activity (GO:0016491)
	6.2	4.3	4.4	iron ion binding (GO:0005506)
	5.7	4.9	3.2	catalytic activity (GO:0003824)
	5.5	2.5	5.2	2 iron, 2 sulfur cluster binding (GO:0051537)
	4.9	2.1	4.8	ferric iron binding (GO:0008199)
	4.0	4.6	1.1	CoA-transferase activity (GO:0008410)
	3.6	1.7	3.4	metal ion binding (GO:0046872)
	2.9	3.2	0.91	ATPase activity (GO:0016887)
	2.7	2.8	1.0	iron-sulfur cluster binding (GO:0051536)
	-2.5	-2.7	-1.0	GTPase activity (GO:0003924)
	-2.8	-1.6	-2.3	nucleotide binding (GO:0000166)
	-2.8	-2.1	-1.9	peptidyl-prolyl cis-trans isomerase activity (GO:0003755)
	-3.1	-3.5	-0.95	endonuclease activity (GO:0004519)
	-3.3	-3.0	-1.7	GTP binding (GO:0005525)
	-3.5	-2.8	-2.2	aminoacyl-tRNA ligase activity (GO:0004812)
	-2.2	-3.0	-0.24	oxidoreductase activity, acting on the CH-OH group of donors, NAD or NADP as acceptor (GO:0016616)
	-1.4	-3.0	1.0	porin activity (GO:0015288)
	-4.6	-4.2	-2.3	nucleic acid binding (GO:0003676)
	-5.6	-4.6	-3.3	RNA binding (GO:0003723)
	-12.3	-9.9	-7.4	structural constituent of ribosome (GO:0003735)

Figure 4

GO enrichment analysis based on parametric analysis of gene set enrichment method. Heat map colors represent calculated Z-scores (FDR < 0.05) shown in figure. BP, biological process; CC, cellular component; MF, molecular function.

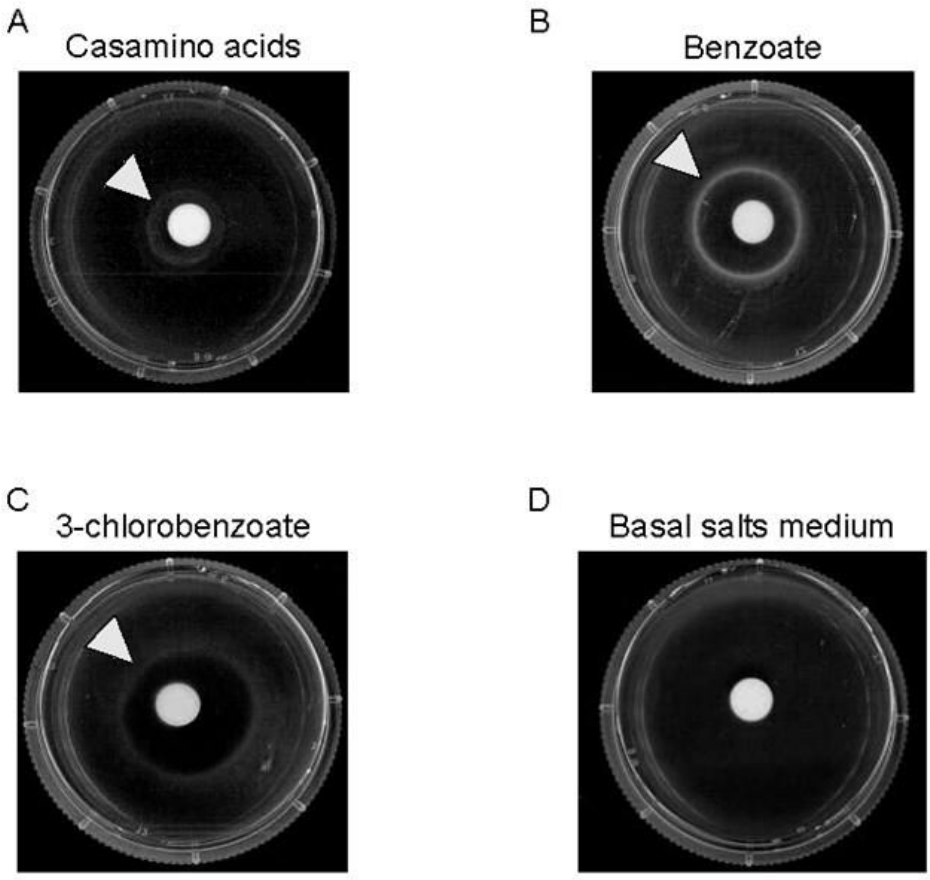

Figure 5

Chemotaxis responses of C. necator NH9 in semi-solid agar plate assay. Chemotaxis of strain NH9 was tested in the presence of casamino acids (A), benzoate (B), 3-chlorobenzoate (C) and basal salts medium (D). Arrows indicate concentric rings, indicative of positive chemotaxis response. All experiments were performed in triplicate.

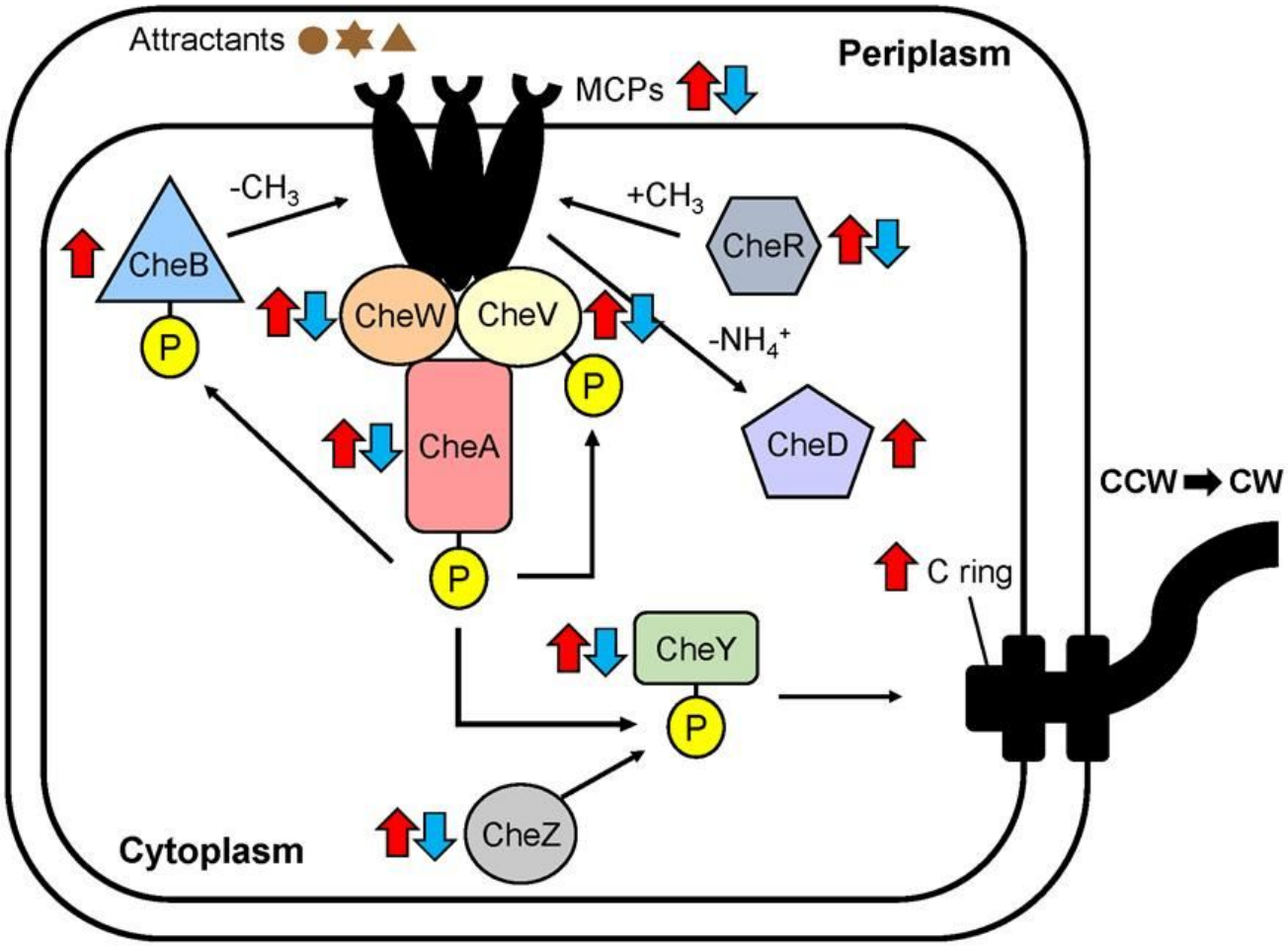

Figure 6

Chemotaxis pathway model of Cupriavidus necator NH9. Detailed predicted chemotaxis pathway of NH9 towards BA. See main text for descriptions of roles of genes encoding MCPs (BJN34_09575, BJN34_21800, BJN34_24350, and BJN34_32190), CheA (BJN34_21875), and CheY (BJN34_21830 and BJN34_21900). CheB (BJN34_21895), CheD (BJN34_21890), and CheR (BJN34_21885) are involved in demethylation, methylation, and deamidation of chemoreceptors, respectively. CheW (BJN34_21835 and BJN34_21880) controls autophosphorylation activity of CheA. CheV (BJN34_33670) functions as a coupling protein, similar to CheW, with additional phosphorylation function. CheZ (BJN34_21905) can dephosphorylate CheY-P. Red arrows indicate genes upregulated more than 2-fold (FDR < 0.05) by BA; blue arrows indicate genes downregulated more than 2-fold (FDR < 0.05) by 3-CB. CCW and CW indicate counterclockwise and clockwise, respectively. One MCP-encoding gene (BJN34_24350) was upregulated by both BA and 3-CB. cheW (BJN34_21835) and cheY (BJN34_21900) showed > 2-fold upregulation (FDR > 0.05) and < 2-fold upregulation, respectively.

Supplementary Files

This is a list of supplementary files associated with this preprint. Click to download.

- TableS8.xlsx
- Sup.Fig.4.pptx
- Sup.Fig.2.pptx
- Sup.Fig.1.pptx
- TableS4revise.xlsx
- TableS6revise.xlsx
- Sup.Fig.3revise.pptx
- TableS2revise.xlsx

- TableS1revise.xlsx
- TableS3revise2.xlsx
- TableS5revise2.xlsx
- TableS7revise2.xlsx